Research Square

Preprints are preliminary reports that have not undergone peer review.
They should not be considered conclusive, used to inform clinical practice,
or referenced by the media as validated information.

Development of Starch–Alginate–PVA Hydrogel Beads for Encapsulation and Sustained Delivery of Trichoderma longibrachiatum in Capsicum annuum

Bandana Padhan

miki.bandana@gmail.com

Adamas University

Parswati Sen

Adamas University

Kartik Charan Lenka

M.S Swaminathan Research Foundation

Joyjyoti Das

Adamas University

Research Article

Keywords: Trichoderma longibrachiatum, hydrogel beads, sodium alginate, starch, polyvinyl alcohol, encapsulation, controlled release, antioxidant enzymes, Capsicum annuum, sustainable agriculture

Posted Date: June 30th, 2026

DOI: https://doi.org/10.21203/rs.3.rs-9858130/v1

License: This work is licensed under a Creative Commons Attribution 4.0 International License.
Read Full License

Additional Declarations: No competing interests reported.

Development of Starch–Alginate–PVA Hydrogel Beads for Encapsulation and Sustained Delivery of *Trichoderma longibrachiatum* in *Capsicum annuum.*

Bandana Padhan[1*], Joyjyoti Das[1*], Parswati Sen[1], Kartik Charan Lenka[2]

[1]Department of Biotechnology, School of Life science and Biotechnology, Adamas University, Kolkata 700126, India

[2]M. S. Swaminathan Research Foundation, Jeypore, Odisha, 764002, India.

[*] Authors to whom correspondence should be addressed.

Corresponding authors

miki.bandana@gmail.com (Bandana Padhan)

jjd.0007@gmail.com (Joyjyoti Das)

Abstract

The development of sustainable microbial delivery systems is essential for improving the efficiency and stability of bioinoculants in agricultural applications. In the present study, a biodegradable sodium alginate–starch–polyvinyl alcohol (PVA) hydrogel system was developed for encapsulation of *Trichoderma longibrachiatum* using the ionic gelation method. The prepared hydrogel beads were characterized for their physicochemical, morphological, and structural properties to evaluate their suitability as controlled-release carriers for fungal bioinoculants. The encapsulated beads exhibited uniform spherical morphology, high moisture retention, enhanced swelling behavior, and high encapsulation efficiency. Scanning electron microscopy revealed porous and interconnected surface architecture favorable for water diffusion and gradual microbial release. FTIR and XRD analyses confirmed successful polymer blending, intermolecular interactions, and the predominantly amorphous nature of the hydrogel matrix.The encapsulated formulation maintained high fungal viability during storage and demonstrated sustained release of viable propagules into soil over time. The plant growth-promoting efficacy of the encapsulated *Trichoderma* formulation was evaluated using *Capsicum annuum* under pot culture conditions and compared with slurry and untreated control treatments. Plants treated with encapsulated hydrogel beads showed significant improvement in morphological parameters, including plant height, leaf number, leaf area, and biomass accumulation. Enhanced stomatal characteristics and increased chlorophyll and carotenoid contents indicated improved photosynthetic performance in treated plants. In addition, encapsulated *Trichoderma* significantly reduced reactive oxygen species and lipid peroxidation while enhancing antioxidant enzyme activities, including superoxide dismutase, catalase, ascorbate peroxidase, and guaiacol peroxidase. The reduction in oxidative stress was accompanied by increased protein accumulation and improved physiological stability. The results demonstrate that the sodium alginate–starch–PVA hydrogel system provides an efficient and eco-friendly platform for sustained delivery of *Trichoderma* inoculants. The synergistic interaction between the biodegradable polymer matrix and fungal bioinoculant improved microbial survival, controlled release behavior, antioxidant defense, and plant

growth promotion, highlighting its potential application in sustainable agriculture and environmentally friendly crop production systems.

Keywords: *Trichoderma longibrachiatum*; hydrogel beads; sodium alginate; starch; polyvinyl alcohol; encapsulation; controlled release; antioxidant enzymes; *Capsicum annuum*; sustainable agriculture

1. Introduction

The increasing global demand for sustainable agricultural production, coupled with the environmental concerns associated with excessive use of chemical fertilizers and pesticides, has accelerated the search for eco-friendly alternatives capable of improving crop productivity while preserving soil health. Beneficial microorganisms have emerged as important biological tools in sustainable agriculture because of their ability to enhance nutrient availability, suppress plant pathogens, and improve plant stress tolerance. Among them, *Trichoderma* species are considered one of the most effective plant growth-promoting fungi owing to their multifunctional role in biological control, rhizosphere colonization, and stimulation of plant growth and defense responses [1].

Trichoderma spp. improve plant performance through several interconnected mechanisms. These fungi exhibit strong antagonistic activity against phytopathogens through mycoparasitism, secretion of hydrolytic enzymes, production of antifungal metabolites, and competition for nutrients and ecological niches [2]. In addition, *Trichoderma* enhances nutrient acquisition by solubilizing phosphate and improving micronutrient availability through siderophore production. The fungi are also known to produce phytohormones and volatile organic compounds that stimulate root architecture, nutrient uptake, and plant biomass accumulation [3]. Furthermore, *Trichoderma* can induce systemic resistance and enhance antioxidant defense pathways, thereby improving plant tolerance against environmental stress and oxidative damage [4]. Because of these combined beneficial properties, *Trichoderma* has gained considerable attention as a biofertilizer, biostimulant, and biological control agent in modern agriculture.

Despite these advantages, practical application of *Trichoderma*-based formulations in agricultural systems remains challenging because microbial propagules often exhibit poor survival under environmental conditions. Conventional application methods such as slurry inoculation or direct soil incorporation frequently result in rapid decline in fungal viability due to desiccation, ultraviolet radiation, temperature fluctuations, and competition with indigenous soil microorganisms [5]. Consequently, the long-term effectiveness of microbial inoculants becomes limited under field conditions. Therefore, development of advanced delivery systems capable of protecting microbial cells and ensuring sustained release in the rhizosphere is essential for improving the agricultural performance of fungal bioinoculants [6].

Encapsulation technology has recently emerged as an effective strategy for enhancing the stability, viability, and controlled release of beneficial microorganisms. Encapsulation involves entrapping viable microbial cells within a polymeric matrix that protects them from adverse environmental conditions while enabling gradual release into soil [7]. Among various encapsulating materials, sodium alginate has been extensively investigated because of its biocompatibility, biodegradability, non-toxicity, and mild ionic gelation properties. However, alginate-only beads often suffer from poor mechanical stability, excessive shrinkage during drying, and rapid degradation under environmental conditions. To overcome these limitations, several studies have explored composite polymeric systems containing additional biopolymers and synthetic polymers for improved structural integrity and sustained release performance.

Recent studies have demonstrated the effectiveness of polymer-assisted encapsulation systems for *Trichoderma* delivery. Alginate–gelatin systems enhanced moisture retention and conidial stability during storage [6, 8]. The incorporation of starch into alginate systems improves porosity, water retention capacity, swelling characteristics, and controlled-release behavior, all of which are critical for sustained microbial delivery in agricultural soils [9]. Nevertheless, reports on starch–alginate–PVA composite hydrogel systems specifically designed for *Trichoderma* encapsulation remain comparatively limited.

In the present study, a biodegradable sodium alginate–starch–PVA hydrogel system was developed for encapsulation of *Trichoderma longibrachiatum* using ionic gelation. The prepared hydrogel beads were characterized for their physicochemical, morphological, and structural properties, including swelling behavior, encapsulation efficiency, SEM, FTIR, and XRD analysis. Furthermore, the viability, storage stability, and controlled-release behavior of the encapsulated fungal propagules were evaluated. The plant growth-promoting efficacy of the encapsulated formulation was assessed in *Capsicum annuum* through analysis of morphological growth parameters, stomatal traits, photosynthetic pigments, reactive oxygen species, antioxidant enzyme activities, and protein accumulation. The study highlights the synergistic role of biodegradable polymeric matrices and fungal bioinoculants in developing environmentally sustainable agricultural delivery systems with enhanced microbial stability and prolonged physiological benefits.

2. Materials and Methods

2.1 Materials

Sodium alginate, polyvinyl alcohol (PVA), soluble starch, carboxymethyl cellulose (CMC), glycerol, calcium chloride dihydrate ($CaCl_2 \cdot 2H_2O$), chitosan, glutaraldehyde, dextrose, agar, and other analytical-grade chemicals used in this study were procured from HiMedia Laboratories (India). All reagents and solvents used were of analytical grade and were used without further purification. Potato dextrose agar (PDA) and Potato dextrose broth (PDB) media were prepared manually.

2.2 Microbial Culture and Maintenance

The fungal strain used in this study was *Trichoderma longibrachiatum*, obtained from M. S. Swaminathan Research Foundation, Jeypore, Koraput. The culture was maintained on manually prepared potato dextrose agar (PDA) plates and subcultured periodically to maintain viability and purity. The inoculated PDA plates were incubated at 28 ± 2°C for 5–7 days until sufficient fungal growth and green sporulation were observed. For mass cultivation, actively growing fungal plugs from PDA plates were aseptically transferred into manually prepared potato dextrose broth (PDB) and incubated statically at 28°C for 5–7 days until dense fungal growth and conidial formation were observed. After incubation, fungal spores were harvested from the broth culture using an ultrasonic cell crusher operating at 40 kHz to obtain a homogeneous spore suspension. The resulting spore suspension was used for subsequent encapsulation studies. The approximate spore concentration was adjusted to ~10^7 spores mL^{-1} prior to encapsulation experiments.

2.3 Preparation of *Trichoderma* Encapsulated Hydrogel Beads

Hydrogel beads containing *Trichoderma longibrachiatum* spores were prepared using the ionic gelation method [10–12]. A homogeneous spore suspension of *Trichoderma* (~10^7 spores mL^{-1}) was mixed thoroughly with the optimized sodium alginate–starch–PVA–glycerol polymer solution under aseptic conditions to ensure uniform distribution of fungal spores within the polymer matrix. A 0.5 M calcium chloride ($CaCl_2$) solution was prepared separately and used as the ionic cross-linking solution. The polymer mixture was then loaded into a sterile syringe fitted with an approximately 0.8 mm nozzle. The solution was extruded dropwise from a height of approximately 4–5 cm into the calcium chloride solution under gentle magnetic stirring. Upon contact with the $CaCl_2$ solution, instantaneous ionic gelation occurred due to cross-linking between calcium ions and sodium alginate, resulting in the formation of spherical hydrogel beads. The formed beads were allowed to remain in the cross-linking solution for 30

min to ensure complete curing and structural stabilization. Following gelation, the hydrogel beads were collected by filtration and washed three times with sterile distilled water to remove excess calcium ions and unreacted residues. The washed beads were then air-dried at room temperature (28 ± 2°C) for 24 h until constant weight was achieved. The dried beads were subsequently used for further characterization and controlled release studies. The dried encapsulated beads were subsequently used for characterization, viability analysis, controlled release studies, and plant growth assessment.

2.4 Physicochemical Characterization of Hydrogel Beads

2.4.1 Bead Size and Weight Measurement

The freshly prepared and dried hydrogel beads were characterized based on their diameter and weight. The diameter of randomly selected beads was measured using a digital Vernier caliper, while the weight of fresh and dried beads was determined using an analytical balance. Measurements were carried out in triplicate and the average values were recorded for further analysis.

2.4.2 Moisture Content Analysis

The moisture content of the hydrogel beads was determined by measuring the difference between the fresh and dried weights of the beads. Initially, the freshly prepared beads were weighed (Wf) and subsequently air-dried at room temperature (28 ± 2°C) until constant weight was achieved. The dried beads were then weighed again (Wd). The moisture content of the hydrogel beads was calculated using the following equation:

$$\text{Moisture Content (\%)} = \frac{W_f - W_d}{W_f} \times 100$$

where, W_f= weight of fresh beads; W_d= weight of dried beads

2.4.3 Swelling Ratio Determination

The swelling behavior of the hydrogel beads was evaluated to determine their water absorption capacity. Dried hydrogel beads of known weight (Wd) were immersed in distilled water at room temperature (28 ± 2°C) for 72 h. After immersion, the swollen beads were carefully

removed, excess surface water was gently blotted using filter paper, and the swollen weight (Ws) was recorded immediately.

The swelling ratio of the hydrogel beads was calculated using the following equation:

$$\text{Swelling Ratio (\%)} = \frac{W_s - W_d}{W_d} \times 100$$

where, W_s= weight of swollen beads; W_d= weight of dried beads.

2.4.3 Encapsulation Efficiency

The encapsulation efficiency of *Trichoderma longibrachiatum* spores within the hydrogel beads was determined to evaluate the effectiveness of the encapsulation process. A known quantity of freshly prepared hydrogel beads was crushed aseptically using sterile distilled water with the help of a sterile mortar and pestle to release the entrapped fungal spores from the polymeric matrix. The obtained suspension was serially diluted and plated on potato dextrose agar (PDA) plates for colony-forming unit (CFU) analysis.

The inoculated plates were incubated at 28 ± 2°C for 5–7 days, after which the viable fungal colonies were counted. Encapsulation efficiency was calculated by comparing the number of viable spores recovered from the hydrogel beads with the initial number of spores added to the polymer solution prior to encapsulation.

The encapsulation efficiency (EE) was calculated using the following equation:

$$EE(\%) = \frac{\text{Number of encapsulated viable spores}}{\text{Total number of spores initially added}} \times 100$$

2.5 Morphological Characterization

2.5.1 Optical Microscopy

The morphological characteristics of the prepared hydrogel beads were initially examined using an optical microscope. Fresh and dried *Trichoderma*-encapsulated hydrogel beads were observed under different magnifications to evaluate bead shape, surface appearance, structural uniformity, and distribution of fungal spores within the polymer matrix. The images obtained

were used to assess the overall morphology and integrity of the hydrogel beads after the encapsulation process.

2.5.2 Scanning Electron Microscopy (SEM) Analysis

The surface morphology and microstructural characteristics of the hydrogel beads were analyzed using Scanning Electron Microscopy (SEM). Prior to analysis, the dried hydrogel bead samples were mounted onto aluminum stubs using double-sided conductive carbon tape and sputter-coated with a thin layer of gold to improve electrical conductivity and image resolution. SEM imaging was performed under an accelerating voltage of 10–15 kV at different magnification ranges to evaluate surface texture, porosity, cracks, structural integrity, and homogeneity of the hydrogel matrix. The obtained micrographs were used to investigate the presence of pores and surface irregularities that may influence swelling behavior, encapsulation efficiency, and controlled release of entrapped *Trichoderma* spores. The porous and interconnected surface architecture observed in the hydrogel beads was considered beneficial for gradual microbial release and water diffusion within the polymeric matrix.

2.6 Structural Characterization

2.6.1 X-ray Diffraction (XRD) Analysis

The crystalline nature and structural properties of the prepared hydrogel beads were investigated using X-ray diffraction (XRD) analysis. The diffraction patterns were recorded over an appropriate 2θ scanning range to determine the degree of crystallinity, amorphous characteristics, and possible intermolecular interactions among sodium alginate, starch, PVA, glycerol, and the encapsulated *Trichoderma* spores.

The XRD profile was further analyzed to identify changes in polymer arrangement and structural modifications after hydrogel formation and encapsulation. The presence of broad diffraction peaks indicated the predominantly amorphous nature of the hydrogel matrix, which is considered favorable for swelling behavior, flexibility, and controlled release applications.

2.6.2 Fourier Transform Infrared Spectroscopy (FTIR) Analysis

Fourier Transform Infrared Spectroscopy (FTIR) analysis was performed to identify the functional groups present in the hydrogel beads and to evaluate possible chemical interactions among sodium alginate, starch, PVA, glycerol, and *Trichoderma* spores within the polymeric network. The dried hydrogel bead samples were analyzed over a scanning range of 4000–400

cm^{-1}. The obtained FTIR spectra were used to identify characteristic absorption peaks corresponding to hydroxyl (–OH), carboxyl (–COOH), and other functional groups involved in intermolecular hydrogen bonding and ionic cross-linking within the hydrogel matrix. Shifts in absorption peaks and variations in peak intensity were analyzed to confirm successful polymer blending and encapsulation of *Trichoderma* within the hydrogel system.

2.7 Viability Study of Encapsulated *Trichoderma*

The viability of *Trichoderma longibrachiatum* spores entrapped within the hydrogel beads was evaluated to determine the efficiency of the encapsulation system in preserving microbial survival during storage. The dried hydrogel beads were stored under sterile conditions at room temperature (28 ± 2°C) in airtight containers until further analysis. Viability analysis was carried out at different storage intervals (10, 15, 20, 25, 30, 35, 40, and 45 days). For each interval, a known quantity of dried hydrogel beads was aseptically weighed and gently crushed using a sterile mortar and pestle in sterile distilled water to release the entrapped fungal spores from the polymeric matrix. The resulting suspension was serially diluted up to 10^{-5} dilution using sterile distilled water. Subsequently, 100 µL aliquots from the appropriate dilution were spread plated onto manually prepared potato dextrose agar (PDA) plates under aseptic conditions. The inoculated plates were incubated at 28 ± 2°C for 5–7 days until visible fungal colonies appeared. Following incubation, viable colonies of *Trichoderma* were counted and expressed as colony-forming units per gram of hydrogel beads (CFU g^{-1} bead). The persistence of fungal growth on PDA plates at different storage intervals confirmed the retention of viability of encapsulated *Trichoderma* spores within the hydrogel matrix during the storage period.

2.8 Controlled Release Study of Encapsulated *Trichoderma*

The controlled release behavior of *Trichoderma longibrachiatum* encapsulated hydrogel beads was evaluated under soil conditions to investigate the gradual release of viable fungal spores from the polymeric matrix over time. Dried hydrogel beads containing encapsulated *Trichoderma* spores were introduced into sterile autoclaved soil to eliminate interference from indigenous microbial populations and to ensure that subsequent fungal growth originated exclusively from the released encapsulated spores. The soil samples containing hydrogel beads were incubated at room temperature (28 ± 2°C) under sterile conditions. Soil samples were collected at different sampling intervals (10, 15, 20, 25, 30, 35, 40, and 45 days). At each

sampling interval, approximately 1 g of soil was aseptically collected and suspended in sterile distilled water to obtain a homogeneous soil suspension. The suspension was thoroughly vortexed and serially diluted up to 10^{-6} dilution using sterile distilled water. Subsequently, 100 µL aliquots from appropriate dilutions were spread plated onto manually prepared potato dextrose agar (PDA) plates under aseptic conditions. The inoculated PDA plates were incubated at 28 ± 2°C for 5–7 days to allow fungal growth and colony development. Following incubation, the number of viable fungal colonies was recorded and expressed as colony-forming units per gram of soil (CFU g^{-1} soil). The appearance and gradual increase in fungal colonies over the incubation period confirmed the sustained and controlled release of viable Trichoderma spores from the hydrogel beads. The release profile obtained from CFU enumeration indicated diffusion-mediated gradual release of fungal propagules from the hydrogel matrix, demonstrating the suitability of the encapsulated system for sustained microbial delivery in agricultural applications.

2.9. Pot Experiment for Plant Growth Assessment

The plant growth-promoting potential of *Trichoderma longibrachiatum* encapsulated hydrogel beads was evaluated through a controlled pot experiment using *Capsicum annuum* (green chilli) as the model plant system. Three experimental treatments were designed to compare the effect of free fungal inoculum and encapsulated fungal formulation on plant growth performance. Plastic pots (approximately 15 cm diameter × 12 cm height) were filled with sterile garden soil and maintained under controlled environmental conditions. Each treatment was carried out in triplicate. Equal numbers of healthy *Capsicum annuum* seeds were sown in each pot. The soil used for the experiment consisted of garden soil with adequate drainage and moisture-holding capacity. For T2 treatment, freshly prepared *Trichoderma* slurry was incorporated into the soil prior to sowing, whereas T3 treatment received the prepared *Trichoderma*-encapsulated hydrogel beads. T1 served as the untreated control. All pots were maintained under natural photoperiod conditions with regular irrigation to maintain adequate soil moisture throughout the experimental period. The plants were grown under ambient laboratory conditions (28 ± 2°C) and monitored periodically.

2.9.1 Plant Growth Parameters

Plant growth parameters were evaluated at weekly sampling intervals during the experimental period. At each interval, plants from each treatment were carefully uprooted and analyzed for morphological and physiological characteristics. Different parameters such as shoot length (cm), root length (cm), number of leaves, biomass (g) were evaluated. Fresh biomass was recorded immediately after harvesting using an analytical balance. For dry biomass determination, plant samples were dried at room temperature until constant weight was achieved. Growth parameters obtained from different treatments were compared to evaluate the effectiveness of encapsulated *Trichoderma* hydrogel beads in promoting plant growth.

2.9.2 Chlorophyll Estimation

Total chlorophyll content was estimated spectrophotometrically using fresh leaf tissue. Approximately 0.1 g of fresh leaf sample was homogenized in chilled 80% acetone for pigment extraction. The homogenate volume was adjusted to 2 mL and centrifuged at 3000 rpm for 10 min. The clear supernatant obtained was used for spectrophotometric analysis [13]. Absorbance values were recorded at wavelengths of 645 nm and 663 nm using a UV–Visible spectrophotometer. Chlorophyll content was calculated using the following equations:

$$\text{Chl a} = 22.9(A_{645}) - 4.68(A_{663})$$

$$\text{Chl b} = 12.7(A_{663}) - 2.69(A_{645})$$

$$\text{Total Chlorophyll} = 20.2(A_{645}) + 8.02(A_{663})$$

Carotenoids (µg/ml) = $(1000A_{470} - 3.27[\text{Chl a}] - 104[\text{Chl b}])/227$

The chlorophyll content was expressed as µg mL^{-1} extract.

4.9.3 Measurement of reactive oxygen species in lemongrass:

4.9.3.1 Hydroxyl radical

To determine the production of OH, a deoxyribose assay was performed according Qadir et al., [14]. Fresh leaf samples (0.1 g) were homogenized in 2 ml of 50 mM sodium phosphate buffer pH 7.0 and centrifuged at 22,000×g for 10 minutes at 4°C. A reaction mixture containing 1ml of supernatant, 0.8 ml of 2.5 mM 2-deoxyribose and 0.2 ml of 2 mM $FeSO_4$, was incubated for 1 hour in dark. This was followed by the addition of 1 ml. of 0.25 % thiobarbituric acid prepared in 10 % trichloro acetic acid (TCA). The contents were boiled for 20 minutes and cooled immediately for 20 minutes in an ice bath and centrifuged at 3000×g for 10 minutes. After centrifugation, absorbance was recorded at 532 nm in a spectrophotometer.

4.9.3.2. Super oxide production

Superoxide anion production rate was measured by monitoring the nitrite formation from hydroxylamine in the presence of O_2- as described by Wu et al., [15]. Segment of 0.5g were harvested from the mid section of the flag leaf and were homogenized at 4°c with 3 ml of 65mM potassium phosphate buffer (pH 7.8) containing 1% (w/v) polyvinylpyrrolidone and centrifuged at 5000×g and 4°c for 15 minutes. The supernatant (0.5 ml.) was mixed with 0.5 ml of 65 mM potassium phosphate buffer (pH 7.8) and 0.1 ml of 10 mM hydroxylamine hydrochloride, and then incubated at 25°c for 30 minutes. The incubated solution (1ml) was added to 1 ml of 58 mM 3-aminobenzene soltonicacid and 1 ml of 7 mM 1-naphthylamine, and then further kept at 25°C for 20 minutes. The absorbance was recorded at 530nm. A standard curve was use to calculate the O_2^- production rate from the reaction equation at O_2^- with hydroxylamine. The values of both MDA content and O_2^- production rate were determined.

4.9.3.3. Hydrogen peroxide content

H_2O_2 was measured by the method of Cai et al. [16]. Leaf tissue (0.25 g) was homogenized in 10 ml of 0.1% w/v aquous TCA and centrifuge at 10000 rpm for 30 min at 4°c. The reaction mixture consist of 0.5 ml of leaf extract with 0.5 ml of 100 mM KPO4 buffer and 2 ml of KI reagent (1M KI). Then it was incubated for one hour in dark and subsequently the absorbance was measured at 390 nm. The concentration of H_2O_2 calculated having the standard curve of H_2O_2. Hydrogen peroxide was measured spectrophotometrically after reaction with KI. The blank consist of 0.1% of TCA without leaf extract.

2.9.4 Antioxidant Enzyme Assays and protein content

For this purpose, fresh samples of leaves (500 mg) collected from different treatments were homogenized in 10 mL ice-cold 50 mM potassium phosphate buffer (pH 7.8) containing 1.0 mM EDTA, 1.0 mM ascorbate, 10% (w/v) sorbitol, and 0.1% Triton X-100. The homogenate was centrifuged at 15,000 × g for 20 min at 4°C, and the supernatant obtained was used as crude enzyme extract. All enzymatic analyses were carried out under cold conditions (0–4°C). All these steps were conducted under cold conditions (0-4°C) (Joana Machado, 2023). Total soluble protein concentration in the extract was quantified according to Lowry et al. [17] procedure, using bovine serum albumin as standard. Activities of antioxidant enzymes were spectrophotometrically determined using appropriate standard procedures with minor modification. Superoxide dismutase (SOD; EC 1.15.1.1) activity was determined based on inhibition of photochemical reduction of nitro blue tetrazolium (NBT). Absorbance was measured at 560 nm using a UV–Visible spectrophotometer. One unit of SOD activity was

defined as the amount of enzyme required to inhibit 50% NBT reduction [1]. Catalase (CAT; EC 1.11.1.6) activity was estimated spectrophotometrically by monitoring the decomposition of hydrogen peroxide (H_2O_2). The decrease in absorbance was recorded at 240 nm. Enzyme activity was calculated using the extinction coefficient of H_2O_2 [1]. Ascorbate peroxidase (APX; EC 1.11.1.11) activity was determined by monitoring the oxidation of ascorbate in the reaction mixture. The decrease in absorbance was measured at 290 nm and enzyme activity was calculated using the extinction coefficient for ascorbate oxidation [1]. Guaiacol peroxidase (GPX) activity was determined based on guaiacol oxidation in the presence of hydrogen peroxide. The increase in absorbance due to tetraguaiacol formation was measured at 470 nm [1]. The activity of the enzymes was determined based on the fresh weight of the tissue, and all analyses were repeated three times to ensure consistency. The chosen antioxidant enzymes (SOD, CAT, APX, and GPX) are some of the main players in the ROS scavenging process, an analysis often conducted to determine plant tolerance against environmental stress (Sivasamy et al., 2022).

2.10 Statistical Analysis

All experiments were conducted in triplicate and the obtained data were expressed as mean ± standard deviation (SD). Statistical analysis was performed using one-way analysis of variance (ANOVA) followed by Tukey's multiple comparison test to determine significant differences among treatments. Differences were considered statistically significant at $p \leq 0.05$.

3. Results and Discussion

3.1.1 Morphology of *Trichoderma* encapsulated Hydrogel Beads

The sodium alginate–starch–PVA–glycerol polymer blend successfully formed spherical hydrogel beads through the ionotropic gelation method upon extrusion into calcium chloride solution. When the polymer droplets came into contact with the $CaCl_2$ solution, immediate bead formation was observed, indicating rapid ionic crosslinking between calcium ions and the carboxyl groups of sodium alginate. This rapid gelation process resulted in the formation of mechanically stable hydrogel beads with uniform morphology and good structural integrity. The fabricated hydrogel beads exhibited distinct morphological changes between fresh and dried states (**Figure 1A–D**). Fresh unloaded hydrogel beads appeared translucent white, smooth, and spherical with relatively uniform size distribution (**Figure 1A**). Following drying, the unloaded beads showed a reduction in size and slight surface shrinkage due to dehydration

of the hydrogel matrix (**Figure 1B**). Encapsulation of *Trichoderma longibrachiatum* within the polymer matrix resulted in the formation of green-colored beads owing to the presence of fungal conidia dispersed throughout the hydrogel network (**Figure 1C**). The fresh encapsulated beads retained their spherical morphology and showed good mechanical stability without rupture during handling. After drying, the encapsulated beads exhibited darker coloration, reduced diameter, and increased rigidity along with slight surface irregularities caused by moisture loss and contraction of the polymeric structure (**Figure 1D**).

The observed bead formation and structural stability were mainly attributed to the presence of sodium alginate, which acted as the primary crosslinkable polymer responsible for gel network formation. Calcium ions from the $CaCl_2$ solution interacted with guluronic acid residues of alginate chains, producing an "egg-box" structure that facilitated rapid hydrogel formation and enhanced bead integrity, as extensively documented for alginate-based encapsulation systems [18]. The incorporation of starch and PVA into the alginate matrix further improved the stability and flexibility of the hydrogel system. Starch contributed to enhanced hydrophilicity and water retention properties of the beads, an effect previously demonstrated in alginate-starch composite systems for biofertilizer delivery [19]. The blending of alginate with gelatinized starch increased the complexity of the matrix network through hydrogen bonding interactions, which in turn helped beads retain their spherical shape after drying [18, 19]. Meanwhile, PVA promoted intermolecular hydrogen bonding interactions within the polymer matrix, thereby increasing mechanical strength and reducing structural collapse during drying [20]. Studies have shown that the addition of PVA to alginate-based systems results in a threefold improvement in the shear modulus of the resulting copolymeric hydrogel, owing to the formation of multiple hydrogen bonds between PVA chains and alginate fibers [20].

In addition, glycerol functioned as a plasticizing agent that improved elasticity and flexibility of the hydrogel network. The presence of glycerol minimized excessive brittleness and cracking during dehydration by enhancing polymer chain mobility and moisture retention within the matrix [21]. Research has shown that glycerol and calcium have a synergic effect on the mechanical properties of crosslinked alginate systems, and that calcium and glycerol concentrations exhibit a combined effect that cannot be predicted by studies varying only one parameter [22]. Furthermore, glycerol addition enhances the water retention ability of dried gel beads and increases the proportion of tightly bound water, thereby improving the tolerance of gel beads to drying [21]. The presence of fillers and glycerol in alginate beads has also been

shown to reduce collapse and roundness distortion during the drying process, further contributing to structural preservation [21].

The combined sodium alginate–starch–PVA–glycerol formulation therefore generated a stable and hydrated three-dimensional polymeric network suitable for efficient encapsulation and sustained delivery of *Trichoderma* spores for agricultural applications. The encapsulation of *Trichoderma* spp. in alginate-based beads represents an eco-friendly strategy for promoting sustainable agriculture [7]. The observed morphological characteristics and structural integrity of the fabricated hydrogel beads are consistent with previous reports on alginate-starch-PVA composite systems for the encapsulation of beneficial microorganisms [23].

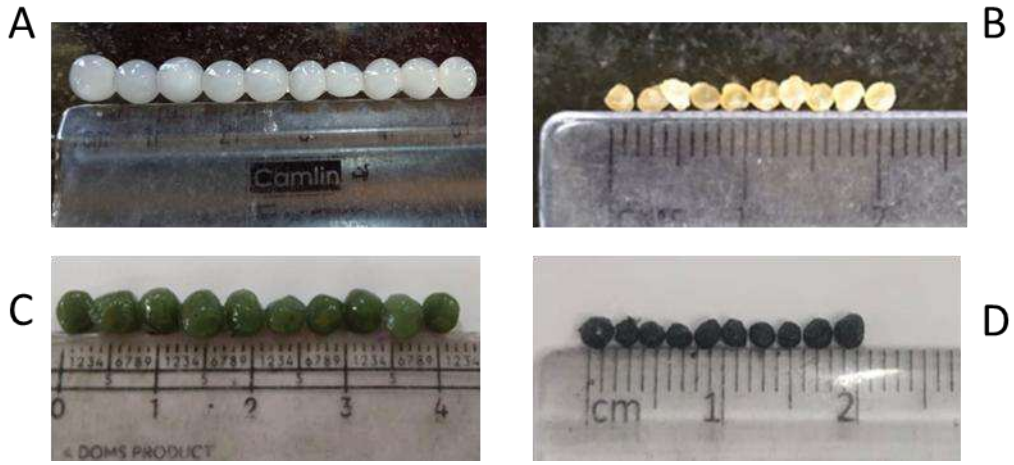

Figure 1 (A–D). Morphological appearance of hydrogel beads at different stages: (A) Fresh unloaded hydrogel beads; (B) Dried unloaded hydrogel beads; (C) Fresh *Trichoderma*-encapsulated hydrogel beads; (D) Dried *Trichoderma*-encapsulated hydrogel beads.

3.2 Physicochemical Characterization of Hydrogel Beads

3.2.1 Bead Diameter and Weight Analysis

The fabricated hydrogel beads exhibited good structural integrity and uniform spherical morphology following calcium-mediated ionic gelation. Comparative analysis between control hydrogel beads (C) and *Trichoderma*-encapsulated hydrogel beads demonstrated noticeable differences in physicochemical characteristics (Figure 2B). The fresh diameter of the encapsulated hydrogel beads was significantly higher (6.0 ± 0.3 mm) than that of the control beads (5.0 ± 0.2 mm), indicating that incorporation of fungal spores and additional polymeric interactions contributed to increased bead size. The increase in size upon encapsulation likely

resulted from the additional solid content and the formation of supplementary intermolecular hydrogen bonds between the fungal cell wall components and the polymer matrix, which expanded the hydrogel network. However, after drying, both formulations exhibited substantial reduction in diameter due to dehydration-induced shrinkage of the hydrogel matrix. The dried control and encapsulated beads exhibited diameters of approximately 0.9 ± 0.05 mm and 1.0 ± 0.04 mm, respectively. Studies have documented that the incorporation of starch as a filler can help maintain bead sphericity and create smooth surfaces on the beads [24]. Starch also acts as a viscosifier that restricts excessive bead swelling while simultaneously improving structural integrity and reducing the porous nature of the alginate network, thereby enhancing the mechanical stability of the beads during drying. The combination of the "egg-box" structure of calcium-crosslinked alginate with the reinforcing effects of starch and PVA resulted in a compact polymeric matrix that, despite experiencing significant volume reduction, maintained its spherical morphology and structural stability without complete collapse [24].

3.2.2 Moisture Content of Hydrogel Beads

Moisture content analysis revealed substantially higher water retention in the *Trichoderma*-encapsulated hydrogel beads compared to the control beads (Figure 2A). The encapsulated hydrogel beads exhibited moisture content of 86.17 ± 1.8%, whereas the control hydrogel beads retained comparatively lower moisture content (63.0 ± 2.1%). The encapsulated hydrogel beads retained approximately 23% higher moisture content than the control beads, indicating that incorporation of *Trichoderma* spores improved the water-holding capacity of the hydrogel matrix. The enhanced moisture retention may be attributed to the hydrophilic nature of sodium alginate, starch, and PVA, whose hydroxyl-rich structures facilitate hydrogen bonding interactions with water molecules. Similarly, SA/CNF/PVA-based hydrogels have been shown to exhibit significantly higher water-retention capacity in both deionized water and mixed soil compared to alginate alone [25]. Furthermore, the sodium alginate–starch–PVA network likely formed a compact and stable matrix capable of retaining higher amounts of bound water [26]. In addition, glycerol acted as an effective plasticizer and moisture-retaining agent that minimized excessive dehydration during drying by stabilizing the polymeric network through hydrogen bonding interactions [21]. High moisture retention is particularly advantageous for microbial encapsulation systems because adequate hydration supports the survival and metabolic stability of entrapped fungal spores during storage and application [12]. Studies on *Trichoderma*-encapsulated granules have demonstrated that the synergistic interaction between

alginate and starch enhances conidial viability during the drying process. The optimized formulation was able to maintain viable cell concentrations above 10^6 CFU/g for up to 14 months under room-temperature storage conditions [12].

3.2.3 Swelling Behavior of Hydrogel Beads

The swelling behavior of the hydrogel beads was evaluated after immersion in distilled water for 72 h, and the encapsulated hydrogel beads exhibited remarkably higher swelling ratio compared to the control beads (Figure 2A). The swelling ratio of the *Trichoderma*-encapsulated hydrogel beads reached 233 ± 5.4%, whereas the control beads exhibited only 61 ± 3.2% swelling. This substantial difference demonstrates that the presence of encapsulated fungal propagules significantly alters the hydration dynamics of the hydrogel matrix. The enhanced swelling behavior may be associated with strong hydrogen bonding interactions among sodium alginate, starch, and PVA, resulting in increased hydrophilicity and water absorption capacity of the hydrogel network. The synergistic effect of these three polymers creates a highly hydrophilic environment with numerous available binding sites for water molecules. Furthermore, the incorporation of glycerol likely enhanced flexibility and porosity of the polymeric matrix, thereby facilitating efficient diffusion and retention of water molecules. Studies on alginate–PVA–glycerol composite hydrogels have documented swelling ratios similar to those observed in the present study, confirming that the ternary polymer system exhibits superior water absorption compared to alginate alone. High swelling capacity is considered highly beneficial for controlled release systems because it promotes gradual diffusion and sustained release of encapsulated microbial propagules into the surrounding soil environment. The swelling behavior also ensures that the beads remain hydrated and functional under fluctuating environmental moisture conditions. Alginate-based encapsulation provides a supportive environment for *T. viride* germination, with mycelia penetrating out of the microspheres. The formulation shows great potential for plant protection and nutrition, offering controlled release and sustained delivery [27]

3.2.4 Encapsulation Efficiency of Trichoderma Spores

The sodium alginate–starch–PVA hydrogel system successfully entrapped viable *Trichoderma longibrachiatum* spores within the polymeric matrix, resulting in high encapsulation efficiency (Figure 2C). The encapsulated hydrogel beads demonstrated an encapsulation efficiency of approximately 87.0 ± 2.0%, indicating effective immobilization and stabilization of fungal

propagules during the ionic gelation process. Combined biopolymer matrices provide superior microbial entrapment by offering a stable hydrophilic network that protects the cells during the encapsulation process. [28]. Similarly, a study on alginate–starch interactions by Locatelli et al. [12]confirmed chemical interactions between the alginate matrix and polymers, which stabilize formulations and keep *Trichoderma* viable during production and storage . Ionic gelation is widely used for cell immobilization because of its mild conditions and rapid crosslinking. A study by Lotfalinezhad et al. [29] on alginate-microencapsulated *T. harzianum* used the ionic gelation method and achieved an encapsulation efficiency of 99%, demonstrating the effectiveness of this trapping mechanism. The inclusion of PVA has been shown to increase the mechanical strength of alginate beads, reducing the likelihood of bead rupture during handling and processing, which in turn minimizes spore loss [30]. Starch addition contributes to the formation of a more tortuous network that physically impedes spore escape. The high encapsulation efficiency achieved in this study therefore confirms the suitability of the developed hydrogel formulation as a biodegradable carrier system for sustained delivery and long-term stabilization of beneficial fungal inoculants for agricultural applications.

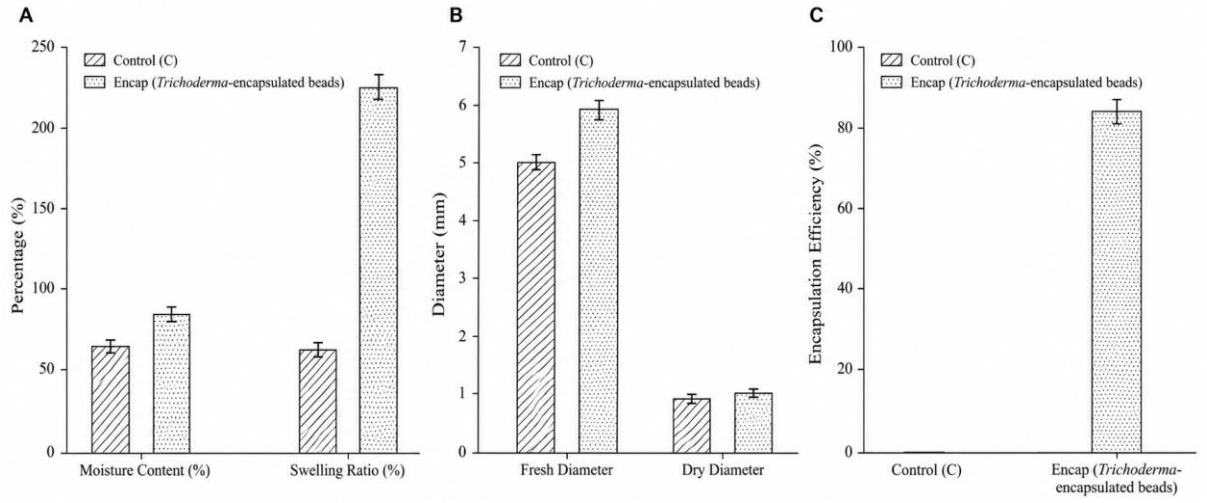

Figure 2. Physicochemical characterization of control hydrogel beads (C) and *Trichoderma*-encapsulated hydrogel beads. (A) Moisture content and swelling ratio of hydrogel beads after 72 h immersion in distilled water; (B) Fresh and dry bead diameter analysis; (C) Encapsulation efficiency of *Trichoderma longibrachiatum* spores within the hydrogel matrix. Data are represented as mean ± standard error (SE) from three independent experiments.

3.3 Morphological Characterization

3.3.1 Scanning Electron Microscopy (SEM) Analysis

Scanning electron microscopy (SEM) analysis was performed to investigate the surface morphology, porosity, and structural characteristics of the developed hydrogel beads at different magnifications (Figure 3). The SEM micrographs revealed that the encapsulated beads possessed a predominantly spherical morphology with a compact outer surface (Figure 3a). The surface appeared relatively smooth at lower magnification, indicating uniform bead formation during the ionotropic gelation process. At intermediate magnification (Figure 3b), the bead surface exhibited fine granular irregularities and micro-roughness, which may enhance water absorption and facilitate interaction with the surrounding environment. Such surface roughness is considered beneficial for rapid hydration and swelling behavior of the hydrogel matrix. Similar findings have been reported for alginate-based systems, where blending with secondary polymers like PVA and starch results in a granular surface topography and influences the release behavior of encapsulated bioactive agents [31]. Studies have also shown that loading with *Trichoderma* spores can reduce microparticle surface roughness, which may contribute to the observed surface features [31]. Higher magnification images (Figure 3c) demonstrated the presence of pores, folds, and localized surface cracks within the polymeric structure. The porous architecture likely originated from solvent evaporation and polymer rearrangement during the drying process [32]. These microstructural features are advantageous for controlled-release formulations, as they facilitate diffusion of water into the matrix and gradual release of encapsulated *Trichoderma* propagules. The observed pore structure may also improve oxygen transfer and moisture retention, thereby supporting spore viability during storage and application. It coincides with the previous studies where it was found that the addition of PVA in polymer blend induces formation of internal pores due to the crystallization of PVA [33].

3.4 Structural Characterization of Hydrogel Beads

3.4.1 X-ray Diffraction (XRD) Analysis

The X-ray diffraction (XRD) patterns of the developed hydrogel beads are presented in Figure X. The diffraction profile exhibited a broad peak centered around $2\theta \approx 19–20°$, indicating the predominantly amorphous nature of the alginate–starch–PVA hydrogel system. The reduction in sharp crystalline peaks suggests that polymer blending disrupted the ordered crystalline

regions of the individual components, resulting in a more homogeneous amorphous matrix. The amorphous characteristics confirm effective intermolecular interactions among sodium alginate, starch, and PVA through hydrogen bonding and polymer chain entanglement [19]. Such structural modification is advantageous for hydrogel-based encapsulation systems because amorphous matrices generally exhibit improved flexibility, swelling capacity, and diffusion behavior compared to highly crystalline materials. In addition to the broad amorphous peak, a distinct sharp diffraction peak was observed around $2\theta \approx 27–28°$, which may be attributed to residual calcium salts or crystalline calcium compounds formed during the ionic cross-linking process with calcium chloride [34]. Similar sharp peaks associated with calcium residues have also been reported in cross-linked alginate-based hydrogels [34].

3.4.2 Fourier Transform Infrared Spectroscopy (FTIR) Analysis

The FTIR spectra of control and *Trichoderma*-encapsulated hydrogel beads were recorded in the 3800–9700 cm^{-1} range (Figure 3-iii). Both formulations exhibited similar spectral profiles, with a broad O–H stretching band (3800–3000 cm^{-1}), aliphatic C–H stretches (3000–2800 cm^{-1}), and a complex fingerprint region (1500–500 cm^{-1}) corresponding to C–O and C–O–C vibrations of alginate, starch, and PVA. The encapsulated beads showed slightly higher normalized absorbance in the O–H/N–H region (1.00 at 3800 cm^{-1} vs. 0.99 in control) and minor variations in the 1500–1000 cm^{-1} region, indicating successful incorporation of fungal biomass. The FTIR spectra of the developed hydrogel beads exhibited characteristic absorption bands confirming the presence of all constituent polymers. The broad absorption band in the 3800–3000 cm^{-1} region is attributed to O–H stretching vibrations of hydroxyl groups from sodium alginate, starch, PVA, and glycerol. Specifically, the hydroxyl stretching band of PVA and sodium alginate typically appears around 3233 cm^{-1}. The peaks observed in the 3000–2800 cm^{-1} range correspond to aliphatic C–H stretching from the PVA backbone and the carboxyl groups of alginate. The presence of these characteristic peaks collectively confirms the successful incorporation of all polymer components into the hydrogel matrix. Comparison of the control and encapsulated bead spectra reveals subtle but significant differences, particularly in the O–H/N–H stretching region (3800–3000 cm^{-1}). The slightly higher absorbance in the encapsulated formulation is attributed to the additional N–H stretching contributions from chitin and proteins present in the *Trichoderma longibrachiatum* conidia cell walls. Similarly, a previous study on alginate-based encapsulation systems for *Trichoderma* species reported intermolecular interactions between alginate functional groups and the polymer matrix, confirming successful encapsulation and stabilization of fungal propagules [35]. Similar FTIR-

based interactions between *Trichoderma* and alginate microspheres were previously reported by Lotfalinezhad et al. [36], where FTIR analysis confirmed interactions between *T. harzianum* and alginate microcapsules following ionic gelation encapsulation. The presence of characteristic functional groups of each polymer component, along with evidence of successful *Trichoderma* spore encapsulation without adverse chemical interactions, validates the suitability of the developed formulation for agricultural bioinoculant delivery applications [12].

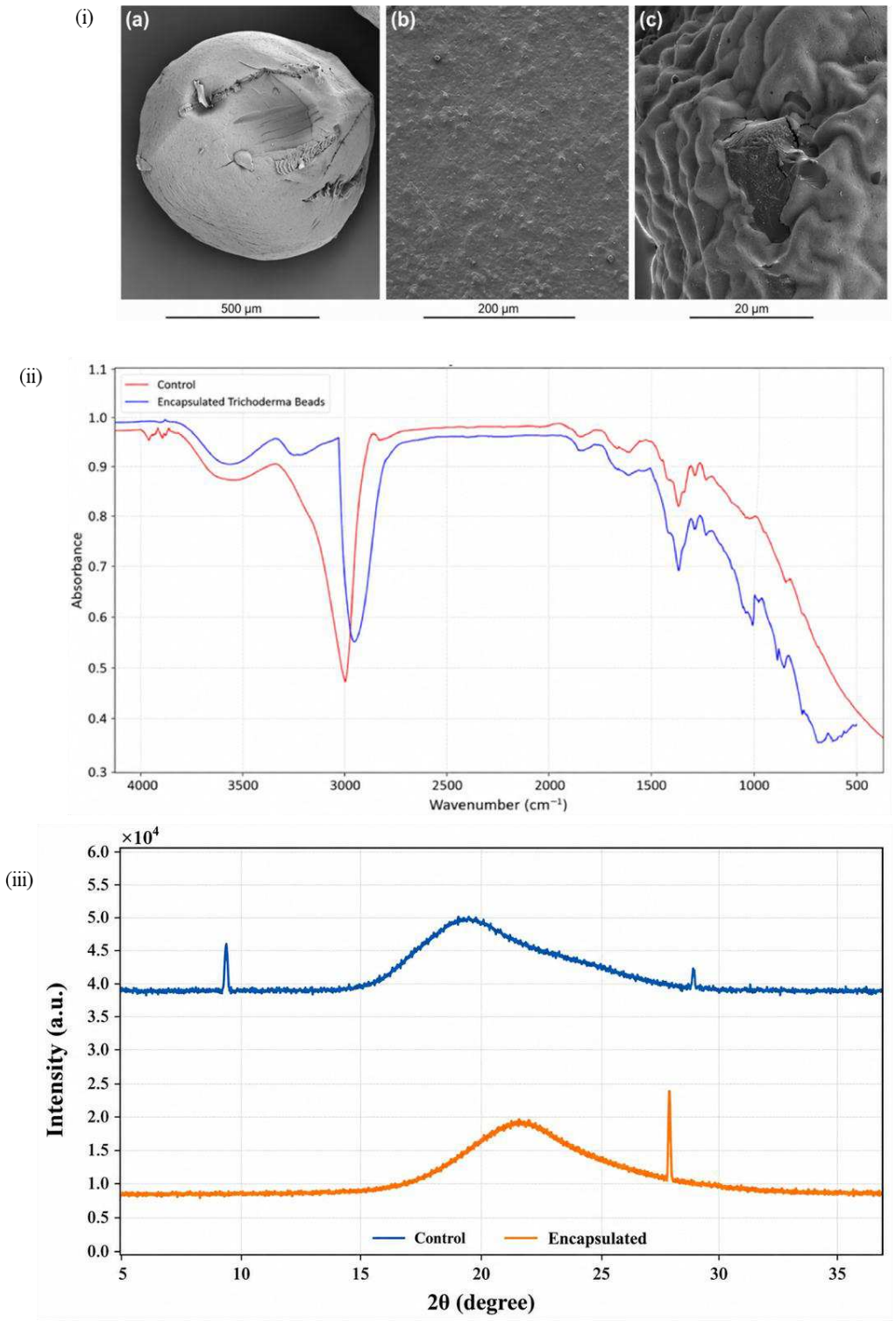

Figure 3. Morphological and structural characterization of encapsulated Trichoderma hydrogel beads: (i) SEM micrographs showing (a) overall bead morphology, (b) surface morphology, and (c) internal porous structure; (ii) FTIR spectra of control and encapsulated *Trichoderma* beads indicating characteristic peak shifts and intermolecular interactions after encapsulation; and (iii) XRD patterns demonstrating structural modification and reduced crystallinity of the encapsulated beads compared to the control sample.

3.5 Storage Stability and Viability Analysis of Encapsulated *Trichoderma*

Results

The storage stability of encapsulated *Trichoderma longibrachiatum* was evaluated by determining viable fungal counts (CFU g^{-1} bead) during storage. The encapsulated hydrogel beads maintained high fungal viability throughout the experimental period, indicating effective preservation of fungal propagules within the polymer matrix. The viable count was recorded as $8.7 \pm 0.03 \times 10^7$CFU g^{-1} bead on Day 10, which gradually decreased to $8.4 \pm 0.02 \times 10^7$on Day 25 and $8.3 \pm 0.02 \times 10^7$CFU g^{-1} bead on Day 35. The minimal reduction in viability demonstrates the ability of the hydrogel formulation to maintain fungal survival during prolonged storage. The sustained viability of encapsulated *Trichoderma* may be attributed to the protective effect of the alginate–starch–PVA hydrogel matrix, which provided a favorable microenvironment for fungal survival. The moisture-retaining nature of the hydrogel likely reduced desiccation stress and maintained metabolic stability of the fungal propagules during storage. In addition, the hydrogen-bonded polymeric network and calcium-mediated crosslinking contributed to structural stability, thereby protecting the encapsulated spores from environmental fluctuations [37]. Previous studies have similarly demonstrated that alginate-based encapsulation effectively preserves the viability and structural stability of *Trichoderma* spp., with capsules maintaining viability above 1×10^7 CFU mL^{-1} for all species during long-term storage [37]. Locatelli et al. [12] further reported that alginate-starch interactions confer greater conidial viability during drying, and the optimal formulation retained viable cell concentrations above 10^6 CFU/g for up to 14 months at room temperature [12]. Lopes et al. [8] showed that freeze-dried alginate beads stored at 8 °C attained viable cell concentrations of 3.0×10^8 CFU/g after 120 days, and FTIR analysis confirmed interactions between alginate and the fungal cell wall, reinforcing the protective role of the matrix. The high viable counts observed even after 45 days in the present study (8.0×10^7 CFU/g) indicate that the developed hydrogel beads are suitable for long-term storage and agricultural bioinoculant applications.

3.6 Controlled Release Behavior of Encapsulated *Trichoderma*

The controlled release behavior of encapsulated *Trichoderma longibrachiatum* was evaluated by estimating viable fungal populations released into soil. The hydrogel beads exhibited gradual release of viable spores over time, confirming sustained microbial delivery from the polymer matrix. The viable count in soil increased from $2.8 \pm 0.15 \times 10^6$CFU g^{-1} soil on Day 10 to $6.2 \pm 0.18 \times 10^6$CFU g^{-1} soil on Day 25 and further reached $7.8 \pm 0.18 \times 10^6$CFU g^{-1} soil on Day 35. The progressive increase in fungal population indicates continuous release of viable propagules from the swollen hydrogel network into the surrounding soil environment. The gradual increase in fungal population within the soil suggests a diffusion-mediated release mechanism from the hydrogel beads. Upon exposure to soil moisture, swelling of the alginate–starch–PVA matrix likely facilitated pore expansion and enhanced diffusion of encapsulated spores into the surrounding medium. Studies on alginate-based encapsulation have demonstrated that conidial release is influenced by exposure time, with the highest release typically observed under neutral pH conditions [37]. The sustained increase in soil CFU counts observed over the 45-day period is consistent with previous findings that *Trichoderma* is gradually released from polymer matrices, with populations reaching a maximum within 30 days and remaining viable for extended periods [38]. The release of active fungi from formulated preparations to soil is known to be governed by factors such as soil pH, moisture content, and the entrapped biomass content [38]. Encapsulating *Trichoderma* spores in a polysaccharide matrix provides a protective environment that ensures their viability and facilitates their controlled release into the soil [7]. The controlled release profile further demonstrates the suitability of the developed hydrogel formulation as an efficient carrier system for microbial bioinoculants, with potential for prolonged biocontrol activity and plant growth promotion in field applications.

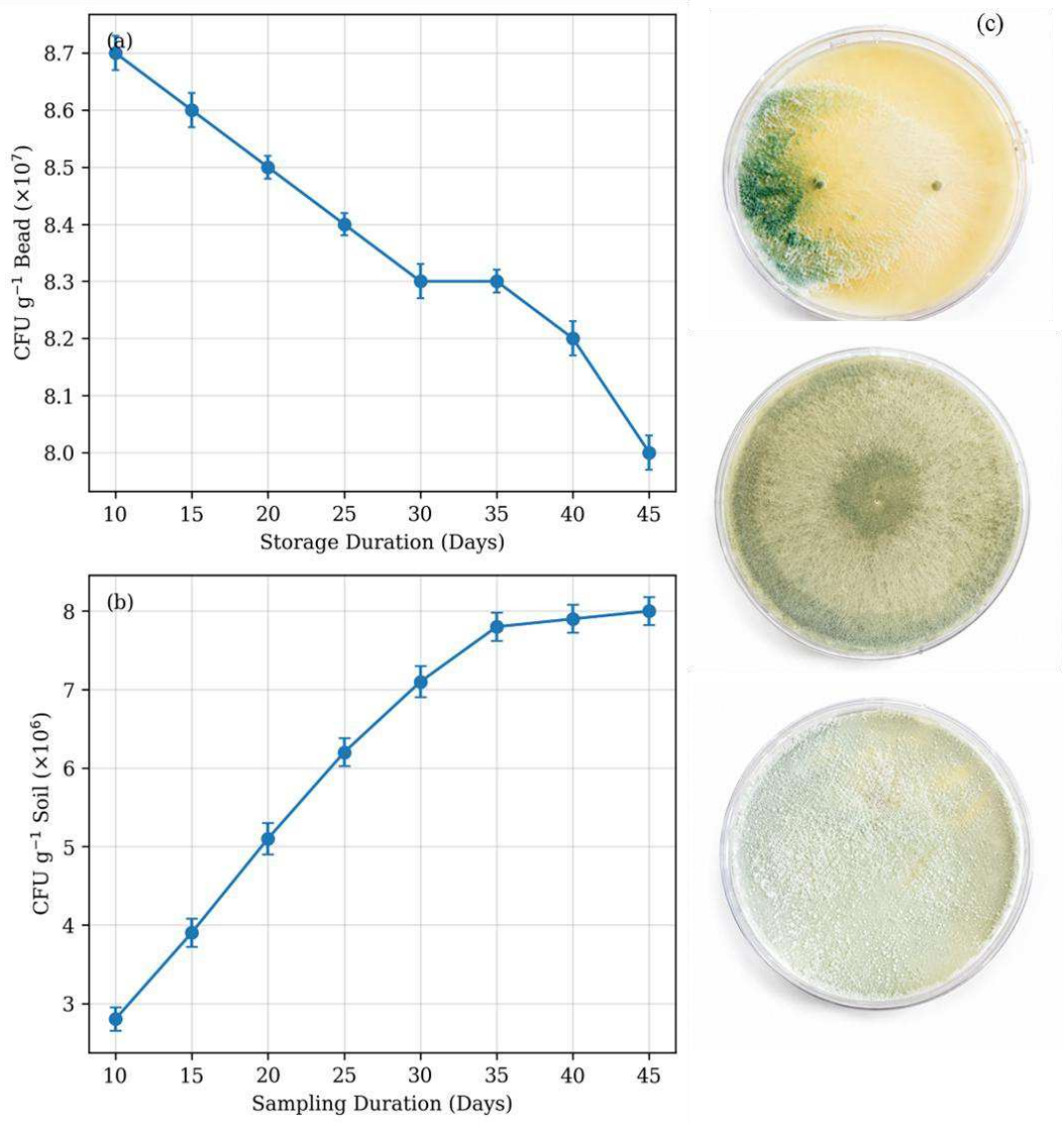

Figure 4. Viability, controlled release behavior, and cultural characteristics of encapsulated *Trichoderma longibrachiatum*. (a) Storage stability profile showing sustained viability of encapsulated fungal propagules during 45 days of storage, expressed as CFU g^{-1} bead. (b) Controlled release profile demonstrating gradual diffusion-mediated release of viable spores into soil over 45 days, expressed as CFU g^{-1} soil. (c) Morphological growth characteristics of released *Trichoderma* colonies on PDA medium confirming successful recovery and viability of encapsulated fungal spores after release from the hydrogel matrix.

3.6 Plant Growth Promotion Study in *Capsicum annuum*

3.6.1 Effect on Morphological Growth Parameters

The application of different treatments significantly influenced the morphological growth parameters of the plants at 10, 20, and 30 days after treatment. Plant height increased

progressively with the advancement of growth stages in all treatments. The different treatments significantly influenced plant morphological parameters throughout the experimental period. Among the treatments, T3 consistently exhibited superior performance, followed by T2, while T1 recorded the lowest values. Plant height, leaf number, leaf area, and dry biomass increased progressively from 10 to 30 days after treatment. At 30 days, T3 recorded the maximum plant height (72.3 ± 3.0 cm), number of leaves (98.4 ± 3.4), leaf area (56.8 ± 2.7 cm^2), and dry weight (18.9 ± 0.5 g), which were significantly higher than T1 (Fig 5(A-D). The enhanced growth observed in T2 and T3 may be attributed to improved nutrient uptake, enhanced physiological activity, and increased photosynthetic efficiency, leading to greater biomass accumulation and vegetative development. The statistically similar responses between T2 and T3 in several parameters indicate their positive role in promoting plant growth, although T3 consistently demonstrated comparatively higher efficacy. The enhancement in plant height, leaf number, and dry weight under T2 and T3 is attributed to the production of the auxin phytohormone indole-3-acetic acid (IAA) by *Trichoderma*, which stimulates cell division, elongation, and overall plant development [39]. Furthermore, *Trichoderma* species can solubilize soil nutrients, particularly phosphate, making them more available to plants, and produce siderophores that chelate iron, thereby improving micronutrient acquisition. These combined effects directly contribute to the enhanced root and shoot growth observed in the treated plants [40]. The observed improvements in plant growth and biomass align with the established multifunctional mechanisms by which *Trichoderma* species promote plant development. The superior performance of encapsulated *Trichoderma* (T3) over both the control and the slurry treatment (T2) highlights the advantages of this delivery system.

3.6.2 Effect on stomatal traits

Different treatments significantly affected stomatal and leaf physiological parameters at 10, 20, and 30 days after treatment. All parameters, including stomatal density (SD), stomatal size (SS), specific leaf area (SLA), and stomatal index (SI), increased progressively with plant growth. Among the treatments, T2 consistently recorded the highest values, followed by T3, while T1 showed the lowest performance. At 10 days, T2 showed maximum SD (328.6 ± 11.2), SS (402.1 ± 8.6), SLA (0.049 ± 0.003), and SI (6.5 ± 0.4), indicating enhanced stomatal development compared to T1. Similar trends were observed at 20 and 30 days, where T2 maintained significantly higher values for all parameters. At 30 days, the highest SD (628.0 ± 12.6), SS (506.2 ± 9.3), SLA (0.076 ± 0.003), and SI (8.5 ± 0.7) were observed in T2 (Fig 5(E-H). The increased stomatal density, stomatal index, and leaf area in treated plants suggest

improved gas exchange, photosynthetic activity, and nutrient utilization. T3 also improved the parameters compared to T1, although the effect was lower than T2. Overall, the results indicate that T2 was most effective in enhancing stomatal characteristics and leaf physiology, thereby promoting better plant growth and physiological efficiency. A study on soybean plants reported that inoculation with *Trichoderma* spp. induced an increase in the stomatal index on the abaxial leaf surface, as well as an increase in the thickness of the mesophyll and the spongy parenchyma [41]. Similarly, in tomato plants subjected to low-temperature stress, inoculation with *Trichoderma asperellum* was found to increase leaf stomatal density indices [42].

3.6.3 Effect on Leaf pigment content

The application of *Trichoderma longibrachiatum* significantly enhanced the photosynthetic pigment content of tomato plants at 10, 20, and 30 days after treatment (DAT). Both slurry (T2) and encapsulated bead formulations (T3) recorded significantly higher chlorophyll and carotenoid concentrations compared to the untreated control (T1), with T3 consistently exhibiting the highest values. At 10 DAT, chlorophyll a increased from 1.84 ± 0.09 mg g^{-1} fwt in T1 to 2.42 ± 0.10 mg g^{-1} fwt in T3, while total chlorophyll increased from 2.46 ± 0.11 to 3.36 ± 0.12 mg g^{-1} fwt. Carotenoid content also increased markedly in treated plants. Similar trends were observed at 20 and 30 DAT, where T3 recorded the maximum chlorophyll a (3.45 ± 0.17 mg g^{-1} fwt), total chlorophyll (4.71 ± 0.20 mg g^{-1} fwt), and carotenoids (0.256 ± 0.02 mg g^{-1} fwt) (Fig. 5 (I-L).

The observed pigment enhancement is consistent with established *Trichoderma* mechanisms. The significant elevation in chlorophyll a, chlorophyll b, and carotenoids in T2 and T3 aligns with reports of *Trichoderma* spp. increasing the synthesis of these pigments [43]. Specifically, *Trichoderma* enhances the uptake of essential macro (P, K, Ca) and micronutrients (Zn, Fe, B), and produces phytohormones like IAA, which influences plant development [44]. The superior performance of the encapsulated treatment (T3) over the slurry (T2) at later intervals likely results from the alginate-starch-PVA matrix providing a protective environment and facilitating controlled conidial release into the soil [7], a system known to promote more sustained physiological benefits [37]. The elevated chlorophyll content directly correlates with improved photosynthetic activity, which is strongly associated with increased plant height, leaf number, leaf area, and biomass [7]. Thus, the enhanced pigment profile in T3 demonstrates the viability of this encapsulated formulation as an effective tool for sustainable

agriculture, capable of delivering prolonged physiological benefits beyond a single slurry application.

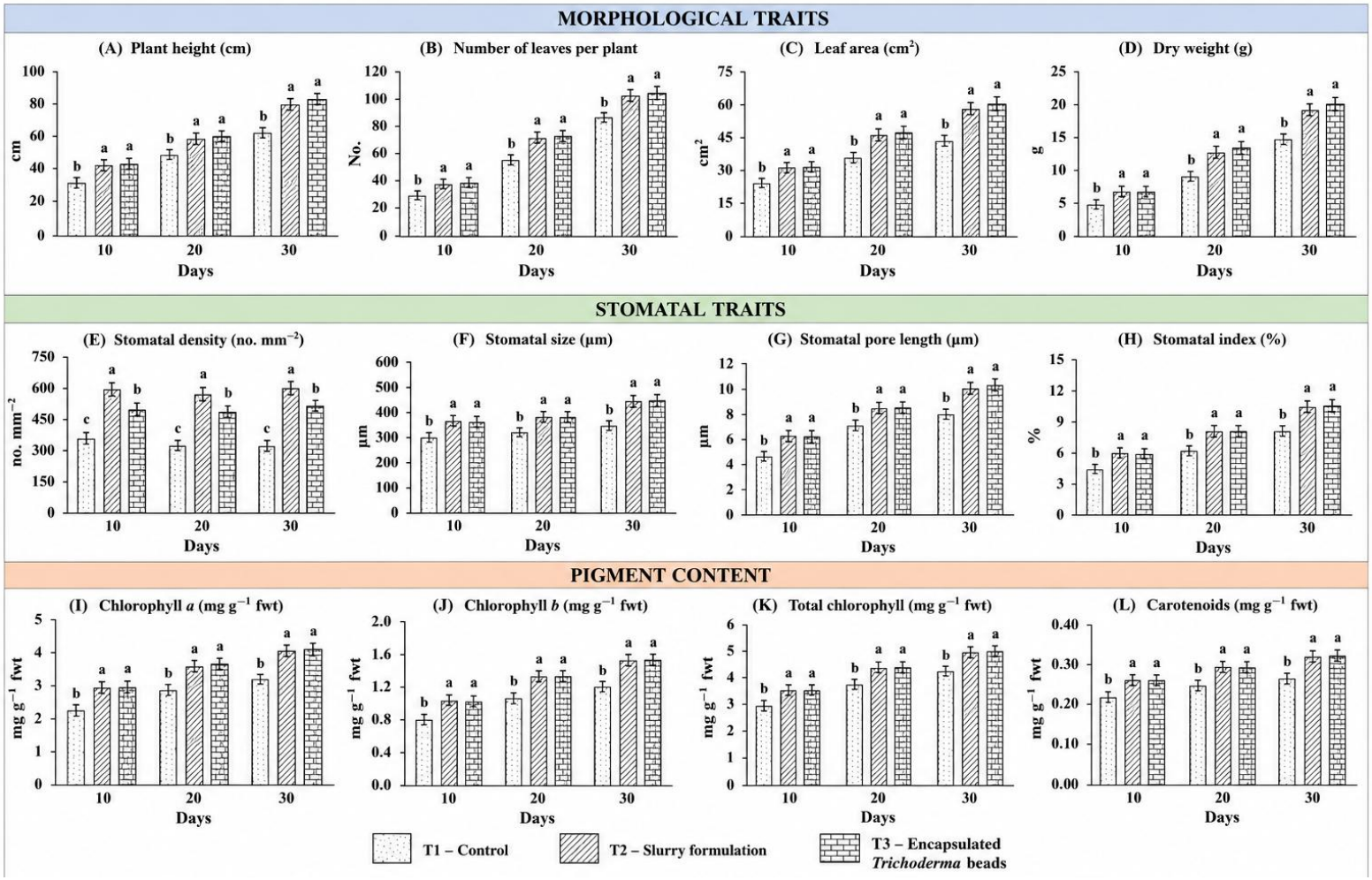

Figure 5. Effect of different Trichoderma formulations on morphological traits, stomatal characteristics, and pigment content of Capsicum annuum at 10, 20, and 30 days after treatment. Morphological parameters included (A) plant height, (B) number of leaves per plant, (C) leaf area, and (D) dry weight. Stomatal traits included (E) stomatal density, (F) stomatal size, (G) stomatal pore length, and (H) stomatal index. Pigment analysis included (I) chlorophyll a, (J) chlorophyll b, (K) total chlorophyll, and (L) carotenoid content. T1 represents control plants, T2 represents slurry formulation-treated plants, and T3 represents encapsulated Trichoderma bead-treated plants. Values are presented as mean ± standard deviation (n = 3). Different letters above bars indicate significant differences among treatments at $p \leq 0.05$.

3.6.4 Levels of reactive oxygen species in plants

The changes in reactive oxygen species (ROS) and lipid peroxidation in *Capsicum annuum* plants grown in soil supplemented with *Trichoderma* hydrogel beads, *Trichoderma* slurry, and control treatments are presented in Table 1. Lipid peroxidation status in plants under different treatments was assessed by measuring the MDA content. Compared with the control treatment (T1), a significant reduction in MDA levels was observed in plants treated with *Trichoderma* slurry (T2) and *Trichoderma* hydrogel beads (T3) at all sampling intervals (10, 20, and 30 days) ($p < 0.05$). At 10 days, the MDA content decreased from 1.84 mM TBA g^{-1} fwt. in T1 to 0.84 mM TBA g^{-1} fwt. in T3, indicating nearly a 2.2-fold reduction. Similarly, lower MDA levels were maintained in T3 at 20 and 30 days, suggesting reduced membrane lipid peroxidation and oxidative damage in treated plants.

The ROS parameters, including superoxide radical (O_2^-), hydrogen peroxide (H_2O_2), and hydroxyl radical (OH^-), also exhibited significant differences among treatments. The superoxide radical content was significantly reduced in *Trichoderma*-treated plants compared to the control. At 10 days, O_2^- content decreased from 0.121 mM g^{-1} fwt. in T1 to 0.081 mM g^{-1} fwt. in T3. Similar declining trends were observed at 20 and 30 days. Hydrogen peroxide content also decreased significantly under *Trichoderma* treatments, with the lowest value recorded in T3 (12.3 mM g^{-1} fwt.) at 30 days compared to T1 (14.5 mM g^{-1} fwt.). Likewise, the hydroxyl radical (OH^-) content showed a marked reduction in treated plants, with T3 consistently recording the lowest values throughout the experimental period. The substantial decrease in malondialdehyde (MDA) content in T2 and T3 treatments is a key indicator of reduced membrane lipid peroxidation. MDA is a well-established biomarker of oxidative membrane damage, and its lower levels suggest that *Trichoderma* protects cell membranes from oxidative attack [45]. Elevated MDA levels typically reflect impaired membrane integrity; conversely, the significant reduction observed in this study indicates superior membrane stability under *Trichoderma* colonization [46].The results indicate that supplementation with *Trichoderma*, particularly in the form of hydrogel beads (T3), effectively reduced oxidative stress in *Capsicum annuum* plants by lowering ROS accumulation and lipid peroxidation. The gradual decline in ROS and MDA levels over time suggests improved antioxidant defense and enhanced cellular protection in treated plants.

Table 1. Changes in reactive oxygen species and lipid peroxidation in *Capsicum annuum* plants grown in soil supplemented with *Trichoderma* hydrogel beads, *Trichoderma* slurry, and control treatments. O_2^-: Superoxide radical; H_2O_2: Hydrogen peroxide; OH^-: Hydroxyl radical; MDA: Malondialdehyde. Data represent the mean ± SD of three replications. Means followed by the same letter are not significantly different at the 5% level according to Duncan's Multiple Range Test (DMRT).

Days	Treatments	O_2^- (mM g^{-1} fwt.)	H_2O_2 (mM g^{-1} fwt.)	OH^- (specific abs. g^{-1} fwt.)	MDA (mM TBA g^{-1} fwt.)
10	T1	0.121 ± 0.005[a]	18.4 ± 0.6[a]	2.46 ± 0.18[a]	1.84 ± 0.09[a]
	T2	0.094 ± 0.004[b]	15.7 ± 0.5[b]	1.86 ± 0.14[b]	1.12 ± 0.06[b]
	T3	0.081 ± 0.003[c]	13.9 ± 0.4[c]	1.42 ± 0.12[c]	0.84 ± 0.05[c]
20	T1	0.102 ± 0.004[a]	16.5 ± 0.5[a]	2.14 ± 0.16[a]	1.43 ± 0.07[a]
	T2	0.086 ± 0.003[b]	14.2 ± 0.4[b]	1.69 ± 0.13[b]	0.96 ± 0.05[b]
	T3	0.079 ± 0.003[c]	12.8 ± 0.4[c]	1.39 ± 0.11[c]	0.71 ± 0.04[c]
30	T1	0.084 ± 0.004[a]	14.5 ± 0.4[a]	1.97 ± 0.18[a]	1.12 ± 0.04[a]
	T2	0.084 ± 0.002[b]	13.0 ± 0.3[b]	1.75 ± 0.12[b]	0.69 ± 0.03[b]
	T3	0.078 ± 0.001[c]	12.3 ± 0.3[c]	1.38 ± 0.10[c]	0.61 ± 0.03[c]

3.6.5 Soluble protein and levels of antioxidant enzyme activity plants

The activities of antioxidant enzymes and protein content in *Capsicum annuum* plants grown in soil supplemented with *Trichoderma* hydrogel beads, *Trichoderma* slurry, and control treatments are presented in Table 2. Significant variations in antioxidant enzyme activities, including superoxide dismutase (SOD), ascorbate peroxidase (APX), guaiacol peroxidase (GPX), catalase (CAT), and total protein content were observed among the treatments throughout the experimental period ($p < 0.05$). The activities of antioxidant enzymes increased significantly in *Capsicum annuum* plants treated with *Trichoderma* formulations compared to the control plants. At 10 days after treatment, SOD activity increased by 36.4% in T3 compared to the control (T1), while APX activity increased by 73.0%. Similarly, GPX and CAT activities increased by 72.2% and 54.9%, respectively, in T3 over T1. Protein content also showed a 49.2% increase in T3 compared to the control plants. A similar trend was observed at 20 and 30 days after treatment. At 30 days, SOD activity increased by 13.2% in T3 compared to T1, whereas APX activity exhibited the highest enhancement with a 149.5% increase. GPX and

CAT activities increased by 14.7% and 21.1%, respectively, while protein content increased by 11.9% compared to the control plants.

The enhanced activities of antioxidant enzymes in *Trichoderma*-treated plants suggest improved cellular defense mechanisms against oxidative stress. SOD plays a crucial role in scavenging superoxide radicals by converting them into hydrogen peroxide, which is subsequently detoxified by APX and CAT enzymes. The increased GPX activity further contributes to the removal of toxic peroxides and protection of cellular membranes. The elevated protein content observed in treated plants may be associated with improved metabolic activity, enhanced enzyme synthesis, and better physiological performance. Among the treatments, *Trichoderma* hydrogel beads (T3) demonstrated the most pronounced effect in enhancing antioxidant defense and protein accumulation, indicating that encapsulated *Trichoderma* formulations provide prolonged microbial activity and sustained physiological benefits to plants [7]. These findings suggest that *Trichoderma*-based hydrogel formulations can effectively improve oxidative stress tolerance, maintain cellular homeostasis, and promote overall plant growth and vigor in *Capsicum annuum*.

Table 2. Changes in antioxidant enzyme activities and protein content in *Capsicum annuum* plants grown in soil supplemented with *Trichoderma* hydrogel beads, *Trichoderma* slurry, and control treatments. SOD: Superoxide dismutase; APX: Ascorbate peroxidase; GPX: Guaiacol peroxidase; CAT: Catalase. Data represent the mean ± SD of three replications. Means followed by the same letter are not significantly different at the 5% level according to Duncan's Multiple Range Test (DMRT).

Days	Treatments	SOD (Units g^{-1} fwt)	APX (mM Asc min^{-1} g^{-1} fwt)	GPX (µM Guaiacol min^{-1} g^{-1} fwt)	CAT (ΔA min^{-1} g^{-1} fwt)	Protein (mg g^{-1} fwt.)
10	T1	42.6 ± 1.8^{b}	0.74 ± 0.04^{b}	0.18 ± 0.01^{b}	3.24 ± 0.18^{b}	12.8 ± 0.6^{b}
	T2	56.8 ± 2.1^{a}	1.21 ± 0.06^{a}	0.29 ± 0.02^{a}	4.86 ± 0.22^{a}	18.4 ± 0.8^{a}
	T3	58.1 ± 2.0^{a}	1.28 ± 0.06^{a}	0.31 ± 0.02^{a}	5.02 ± 0.24^{a}	19.1 ± 0.7^{a}
20	T1	61.4 ± 2.3^{b}	0.86 ± 0.05^{b}	0.24 ± 0.02^{b}	4.52 ± 0.20^{b}	17.6 ± 0.7^{b}
	T2	73.5 ± 2.6^{a}	1.64 ± 0.08^{a}	0.35 ± 0.02^{a}	6.14 ± 0.25^{a}	22.5 ± 0.9^{a}
	T3	75.2 ± 2.5^{a}	1.72 ± 0.08^{a}	0.36 ± 0.02^{a}	6.32 ± 0.27^{a}	23.1 ± 0.8^{a}
30	T1	75.6 ± 1.5^{b}	0.93 ± 0.11^{b}	0.34 ± 0.02^{b}	5.70 ± 0.56^{b}	21.9 ± 0.7^{b}
	T2	79.2 ± 1.4^{a}	1.57 ± 0.11^{a}	0.37 ± 0.04^{a}	6.30 ± 0.28^{a}	24.0 ± 1.8^{a}

T3	85.6 ± 2.5[a]	2.32 ± 0.30[a]	0.39 ± 0.01[a]	6.90 ± 0.99[a]	24.5 ± 1.8[a]

3.7 Proposed Mechanism of Plant Growth Promotion by Encapsulated *Trichoderma*

The encapsulated *Trichoderma* hydrogel bead system acts as an efficient carrier for the gradual and sustained delivery of fungal inoculants into the rhizosphere, thereby improving plant growth and physiological performance in *Capsicum annuum*. Upon soil application, the hydrogel matrix absorbs water and swells, creating a moist microenvironment favorable for fungal survival and activation [7]. The swollen hydrogel beads gradually release viable *Trichoderma* propagules into the surrounding soil, ensuring prolonged microbial availability and sustained rhizosphere colonization [37]. The released *Trichoderma* effectively colonizes the root surface and rhizosphere region, enhancing root growth and nutrient acquisition [47]. Improved uptake of essential nutrients such as nitrogen, phosphorus, and potassium contributes to increased chlorophyll synthesis, photosynthetic efficiency, and biomass accumulation [39]. In addition, *Trichoderma* is known to produce various plant growth-promoting metabolites, phytohormones, and enzymes that stimulate root development and overall plant vigor [47]

Encapsulated *Trichoderma* treatment also enhanced the antioxidant defense system of the plants by increasing the activities of enzymes such as SOD, APX, GPX, and CAT [48]. Enhanced antioxidant activity reduces the accumulation of reactive oxygen species (ROS) including superoxide radicals, hydrogen peroxide, and hydroxyl radicals, thereby minimizing lipid peroxidation and cellular membrane damage [49]. The reduction in oxidative stress ultimately improves physiological stability and stress tolerance in plants [50]. The hydrogel matrix and fungal inoculant work synergistically to maintain moisture, protect fungal viability, and provide controlled release of bioactive propagules over an extended period [37]. This sustained microbial activity improves soil–root interactions, promotes beneficial rhizosphere processes, and supports continuous plant growth promotion [51]. Therefore, encapsulated *Trichoderma* hydrogel beads represent an effective and eco-friendly strategy for enhancing plant growth, antioxidant defense, and overall crop productivity [7].

4. Conclusion

The developed sodium alginate–starch–PVA hydrogel system successfully encapsulated *Trichoderma longibrachiatum* and demonstrated excellent physicochemical stability, high

encapsulation efficiency, enhanced swelling behavior, and sustained fungal viability during storage and soil application. Structural characterization confirmed the formation of a stable amorphous polymeric network with suitable porosity and mechanical integrity for microbial immobilization and controlled release applications. The encapsulated formulation maintained prolonged fungal survival and enabled gradual diffusion-mediated release of viable propagules into the soil, indicating its effectiveness as a controlled delivery system for agricultural bioinoculants.

Application of the encapsulated *Trichoderma* significantly improved the growth and physiological performance of *Capsicum annuum* plants compared with slurry and untreated control treatments. Enhanced plant height, leaf number, biomass accumulation, stomatal traits, chlorophyll pigments, and carotenoid contents indicated improved photosynthetic efficiency and nutrient utilization. In addition, encapsulated *Trichoderma* effectively reduced reactive oxygen species and lipid peroxidation while increasing antioxidant enzyme activities and protein accumulation, thereby improving oxidative stress tolerance and cellular protection in plants. The hydrogel bead formulation consistently exhibited superior performance over the slurry treatment, highlighting the advantage of sustained microbial release and prolonged rhizosphere colonization. The present study demonstrates that sodium alginate–starch–PVA hydrogel beads are promising biodegradable carrier systems for the encapsulation and controlled delivery of beneficial fungal inoculants. The synergistic interaction between the hydrogel matrix and *Trichoderma* provides sustained physiological benefits, enhanced antioxidant defense, and improved plant growth promotion. Therefore, the developed encapsulated *Trichoderma* formulation has strong potential for sustainable agricultural applications as an eco-friendly biofertilizer and plant growth-promoting system.

Funding Declaration

The authors declare that no funding was received for this research, authorship, and/or publication of this article.

References

1. Padhan B, Lenka KC, Mantry T, et al (2025) Evaluating the Impact of Trichoderma Biostimulants on Eco-physiological Traits Across Diverse Crop Species. Proceedings of the Indian National Science Academy Part B 95:851–860. https://doi.org/10.1007/s40011-025-01734-4

2. Chen X, Lu Y, Liu X, et al (2025) Trichoderma: Dual Roles in Biocontrol and Plant Growth Promotion. Microorganisms 13:1840. https://doi.org/10.3390/microorganisms13081840

3. Tyśkiewicz R, Nowak A, Ozimek E, Jaroszuk-Ściseł J (2022) Trichoderma: The Current Status of Its Application in Agriculture for the Biocontrol of Fungal Phytopathogens and Stimulation of Plant Growth. Int J Mol Sci 23:2329. https://doi.org/10.3390/ijms23042329

4. Zhao L, Zhang Y (2015) Effects of phosphate solubilization and phytohormone production of *Trichoderma asperellum* Q1 on promoting cucumber growth under salt stress. Journal of Integrative Agriculture 14:1588–1597. https://doi.org/10.1016/S2095-3119(14)60966-7

5. Vindas-Reyes E, Chacón-Cerdas R, Rivera-Méndez W (2024) Trichoderma Production and Encapsulation Methods for Agricultural Applications. AgriEngineering 6:2366–2384. https://doi.org/10.3390/agriengineering6030138

6. Arias-Chavarría LD, Batista-Menezes D, Orozco-Cayasso S, et al (2025) Evaluation of the viability of microencapsulated Trichoderma longibrachiatum conidia as a strategy to prolong the shelf life of the fungus as a biological control agent. Front Chem 12:. https://doi.org/10.3389/fchem.2024.1473217

7. Ngulela AI, Bengharez Z, Slamani I, Mahboubi S (2025) Formulation of Alginate- and Pectin-Based Beads Encapsulating Trichoderma for Sustainable and Efficient Agriculture. Chemistry Proceedings 16:64. https://doi.org/10.3390/ecsoc-28-20186

8. Lopes AR de O, Locatelli GO, Barbosa R de M, et al (2020) Preparation, characterisation and cell viability of encapsulated Trichoderma asperellum in alginate beads. J Microencapsul 37:270–282. https://doi.org/10.1080/02652048.2020.1729884

9. Wu Z, Guo L, Qin S, Li C (2012) Encapsulation of R. planticola Rs-2 from alginate-starch-bentonite and its controlled release and swelling behavior under simulated soil conditions. J Ind Microbiol Biotechnol 39:317–327. https://doi.org/10.1007/s10295-011-1028-2

10. Lotfalinezhad E, Taheri A, Razavi SE, Sanei SJ (2024) Preparation and assessment of alginate-microencapsulated Trichoderma harzianum for controlling Sclerotinia sclerotiorum and Rhizoctonia solani on tomato. International Journal of Biological Macromolecules 259:129278. https://doi.org/10.1016/J.IJBIOMAC.2024.129278

11. dos Santos GF, Locatelli GO, Coêlho DA, et al (2015) Factorial design, preparation and characterization of new beads formed from alginate, polyphosphate and glycerol gelling solution for microorganism microencapsulation. J Sol-Gel Sci Technol 75:345–352. https://doi.org/10.1007/s10971-015-3705-5

12. Locatelli GO, dos Santos GF, Botelho PS, et al (2018) Development of *Trichoderma* sp. formulations in encapsulated granules (CG) and evaluation of conidia shelf-life. Biological Control 117:21–29. https://doi.org/10.1016/j.biocontrol.2017.08.020

13. Padhan B, Panda D (2018) Variation of photosynthetic characteristics and yield in wild and cultivated species of yams (Dioscorea spp.) from Koraput, India. Photosynthetica 56:. https://doi.org/10.1007/s11099-018-0823-7

14. Qadir SU, Raja V, Siddiqui WA, et al (2021) Foliar Concentrations of Selected Elements, Assessment of Oxidative Stress Markers and Role of Antioxidant Defense System is Associated with Fly Ash Stress Tolerance in Withania somnifera. J Plant Growth Regul 40:1450–1465. https://doi.org/10.1007/s00344-020-10200-6

15. Wu F, Yang H, Chang Y, et al (2012) Effects of nitric oxide on reactive oxygen species and antioxidant capacity in Chinese Bayberry during storage. Scientia Horticulturae 135:106–111. https://doi.org/10.1016/j.scienta.2011.12.011

16. Cai H, Liu X, Zou J, et al (2018) Multi-wavelength spectrophotometric determination of hydrogen peroxide in water with peroxidase-catalyzed oxidation of ABTS. Chemosphere 193:833–839. https://doi.org/10.1016/j.chemosphere.2017.11.091

17. Lowry OliverH, Rosebrough NiraJ, Farr AL, Randall RoseJ (1951) PROTEIN MEASUREMENT WITH THE FOLIN PHENOL REAGENT. Journal of Biological Chemistry 193:265–275. https://doi.org/10.1016/S0021-9258(19)52451-6

18. Zafeiri I, Beri A, Linter B, Norton I (2021) Mechanical properties of starch-filled alginate gel particles. Carbohydrate Polymers 255:117373. https://doi.org/10.1016/j.carbpol.2020.117373

19. Rohman S, Kaewtatip K, Kantachote D, Tantirungkij M (2021) Encapsulation of Rhodopseudomonas palustris KTSSR54 using beads from alginate/starch blends. Journal of Applied Polymer Science 138:50084. https://doi.org/10.1002/app.50084

20. Zhang R, Zhao W, Ning F, et al (2022) Alginate Fiber-Enhanced Poly(vinyl alcohol) Hydrogels with Superior Lubricating Property and Biocompatibility. Polymers (Basel) 14:4063. https://doi.org/10.3390/polym14194063

21. Wang X, Feng Y, Feng T, et al (2021) Modulation effect of glycerol on plasticization and water distribution of vacuum-dried calcium alginate gel beads encapsulating peppermint oil/β-cyclodextrin complex. Food Bioscience 41:100968. https://doi.org/10.1016/j.fbio.2021.100968

22. Giz AS, Berberoglu M, Bener S, et al (2020) A detailed investigation of the effect of calcium crosslinking and glycerol plasticizing on the physical properties of alginate films. Int J Biol Macromol 148:49–55. https://doi.org/10.1016/j.ijbiomac.2020.01.103

23. Santos-Díaz A, Uribe-Gutiérrez L, Cruz-Barrera M (2022) High-Throughput Assessments for Storage Stability, In Vitro Release, and Particle Size of Encapsulated Biocontrol Fungi in Hydrogel Beads. Current Protocols 2:e486. https://doi.org/10.1002/cpz1.486

24. Chan E-S, Wong S-L, Lee P-P, et al (2011) Effects of starch filler on the physical properties of lyophilized calcium–alginate beads and the viability of encapsulated cells. Carbohydrate Polymers 83:225–232. https://doi.org/10.1016/j.carbpol.2010.07.044

25. S L, Q W, X S, et al (2021) Novel alginate-cellulose nanofiber-poly(vinyl alcohol) hydrogels for carrying and delivering nitrogen, phosphorus and potassium chemicals. International journal of biological macromolecules 172:. https://doi.org/10.1016/j.ijbiomac.2021.01.063

26. Samuel M, Quraishi R, Sahu N, et al (2026) Lignin nanoparticle reinforced polyvinyl alcohol, rice starch water and sodium alginate blend film for food packaging applications. Materials Today Communications 51:114829. https://doi.org/10.1016/j.mtcomm.2026.114829

27. Jurić S, Đermić E, Topolovec-Pintarić S, et al (2019) Physicochemical properties and release characteristics of calcium alginate microspheres loaded with *Trichoderma viride* spores. Journal of Integrative Agriculture 18:2534–2548. https://doi.org/10.1016/S2095-3119(19)62634-1

28. Szopa D, Mielczarek M, Skrzypczak D, et al (2022) Encapsulation efficiency and survival of plant growth-promoting microorganisms in an alginate-based matrix – A systematic review and protocol for a practical approach. Industrial Crops and Products 181:114846. https://doi.org/10.1016/j.indcrop.2022.114846

29. Lotfalinezhad E, Taheri A, Razavi SE, Sanei SJ (2024) Preparation and assessment of alginate-microencapsulated *Trichoderma harzianum* for controlling *Sclerotinia sclerotiorum* and *Rhizoctonia solani* on tomato. International Journal of Biological Macromolecules 259:129278. https://doi.org/10.1016/j.ijbiomac.2024.129278

30. L Z, X M, D L, et al (2022) Encapsulation of Bacillus pumilus G5 from polyvinyl alcohol-sodium alginate (PVA-SA) and its implications in improving plant growth and soil fertility under drought and salt soil conditions. International journal of biological macromolecules 209:. https://doi.org/10.1016/j.ijbiomac.2022.04.017

31. Jurić S, Šegota S, Vinceković M (2019) Influence of surface morphology and structure of alginate microparticles on the bioactive agents release behavior. Carbohydrate Polymers 218:234–242. https://doi.org/10.1016/j.carbpol.2019.04.096

32. Tahir M, Sionkowska A (2023) Effect of Polydopamine and Curcumin on Physicochemical and Mechanical Properties of Polymeric Blends. Materials (Basel) 16:5758. https://doi.org/10.3390/ma16175758

33. Adzmi F, Musa MH, Siddiqui Y, et al (2020) Development of Alginate-Montmorillonite-Starch with Encapsulated Trichoderma harzianum and Evaluation of Conidia Shelf Life. Int J Agric Biol 26:. https://doi.org/10.17957/IJAB/15.1812

34. Khalid I, Ahmad M, Minhas MU, Barkat K (2018) Preparation and characterization of alginate-PVA-based semi-IPN: controlled release pH-responsive composites. Polym Bull 75:1075–1099. https://doi.org/10.1007/s00289-017-2079-y

35. Adzmi F, Meon S, Musa MH, Yusuf NA (2012) Preparation, characterisation and viability of encapsulated Trichoderma harzianum UPM40 in alginate-montmorillonite clay. J Microencapsul 29:205–210. https://doi.org/10.3109/02652048.2012.659286

36. Lotfalinezhad E, Taheri A, Razavi SE, Sanei SJ (2024) Preparation and assessment of alginate-microencapsulated *Trichoderma harzianum* for controlling *Sclerotinia*

sclerotiorum and *Rhizoctonia solani* on tomato. International Journal of Biological Macromolecules 259:129278. https://doi.org/10.1016/j.ijbiomac.2024.129278

37. Pinotti TI, de Paula Taffarel V, de Araújo Silva Cipriano G, et al (2026) Formulation of Trichoderma spp. encapsulated in alginate: potential for biofungicide with controlled conidial release. World J Microbiol Biotechnol 42:277. https://doi.org/10.1007/s11274-026-04989-9

38. Prasad RD, Chandrika KSVP, Godbole V (2020) A novel chitosan biopolymer based *Trichoderma* delivery system: Storage stability, persistence and bio efficacy against seed and soil borne diseases of oilseed crops. Microbiological Research 237:126487. https://doi.org/10.1016/j.micres.2020.126487

39. Contreras-Cornejo HA, Schmoll M, Esquivel-Ayala BA, et al (2024) Mechanisms for plant growth promotion activated by *Trichoderma* in natural and managed terrestrial ecosystems. Microbiological Research 281:127621. https://doi.org/10.1016/j.micres.2024.127621

40. Zhao L, Wang F, Zhang Y, Zhang J (2014) Involvement of Trichoderma asperellum strain T6 in regulating iron acquisition in plants. J Basic Microbiol 54 Suppl 1:S115-124. https://doi.org/10.1002/jobm.201400148

41. Oliveira CM, Almeida NO, Rocha MR da, et al (2020) Anatomical changes induced by isolates of Trichoderma spp. in soybean plants. PLOS ONE 15:e0242480. https://doi.org/10.1371/journal.pone.0242480

42. Osorno-Suárez M del P, Hernández-Soto I, Aquino-Torres E, et al (2025) Trichoderma asperellum Enhances Low-Temperature Tolerance of Tomato Plants by Regulating Oxidative Stress, Osmolyte Accumulation, and Stomatal Traits. Horticulturae 11:1502. https://doi.org/10.3390/horticulturae11121502

43. Soliman M, Alnusaire T, Abdelbaky N, et al (2020) *Trichoderma*-Induced Improvement in Growth, Photosynthetic Pigments, Proline, and Glutathione Levels in *Cucurbita pepo* Seedlings under Salt Stress. PHYTON 89:473–486. https://doi.org/10.32604/phyton.2020.08795

44. Vukelić ID, Prokić LT, Racić GM, et al (2021) Effects of Trichoderma harzianum on Photosynthetic Characteristics and Fruit Quality of Tomato Plants. International Journal of Molecular Sciences 22:6961. https://doi.org/10.3390/ijms22136961

45. Li M, Ma G, Lian H, et al (2019) The effects of *Trichoderma* on preventing cucumber fusarium wilt and regulating cucumber physiology. Journal of Integrative Agriculture 18:607–617. https://doi.org/10.1016/S2095-3119(18)62057-X

46. Rezaloo Z, Aliloo AA, Shahbazi S, Salajoughi M (2022) Physiological response of pinto bean plants (Phaseolus vulgaris) to Trichoderma spp. Inoculants

47. Cruz-Magalhães V, Padilla-Arizmendi F, Hampton J, Mendoza-Mendoza A (2022) Trichoderma Rhizosphere Competence, Suppression of Diseases, and Biotic Associations. In: Horwitz BA, Mukherjee PK (eds) Microbial Cross-talk in the Rhizosphere. Springer Nature, Singapore, pp 235–272

48. Youssef SA, Tartoura KA, Abdelraouf GA (2016) Evaluation of *Trichoderma harzianum* and *Serratia proteamaculans* effect on disease suppression, stimulation of ROS-scavenging enzymes and improving tomato growth infected by *Rhizoctonia solani*. Biological Control 100:79–86. https://doi.org/10.1016/j.biocontrol.2016.06.001

49. Singh BN, Singh A, Singh SP, Singh HB (2011) Trichoderma harzianum- mediated reprogramming of oxidative stress response in root apoplast of sunflower enhances defence against Rhizoctonia solani. Eur J Plant Pathol 131:121–134. https://doi.org/10.1007/s10658-011-9792-4

50. Zheng F, Fu Y, Yu P, et al (2024) Flavonoid synthesis is crucial for *Trichoderma asperellum*-induced systemic resistance to root-knot nematodes in tomato plants. Plant Physiology and Biochemistry 212:108706. https://doi.org/10.1016/j.plaphy.2024.108706

51. Ji Y, Liu S, Zhao Z, et al (2025) Synthetic biology-assisted fungus-assembling beads for regulating rhizosphere microbiome and improving plant growth in saline soil. Environmental Technology & Innovation 40:104343. https://doi.org/10.1016/j.eti.2025.104343